Zhuang *et al. Microbiome* (2025) 13:13
https://doi.org/10.1186/s40168-024-02010-9

Microbiome

RESEARCH

Open Access

Core microbe *Bifidobacterium* in the hindgut of calves improves the growth phenotype of young hosts by regulating microbial functions and host metabolism

Yimin Zhuang[1†], Duo Gao[1†], Wen Jiang[1,2†], Yiming Xu[1,2], Guanglei Liu[1], Guobin Hou[1,4], Tianyu Chen[1], Shangru Li[1], Siyuan Zhang[1,2], Shuai Liu[1], Jingjun Wang[1], Jianxin Xiao[1,3], Mengmeng Li[1], Wei Wang[1], Shengli Li[1] and Zhijun Cao[1*]

Abstract

Background The growth and health of young ruminants are regulated by their gut microbiome, which can have lifelong consequences. Compared with subjective grouping, phenotypic clustering might be a more comprehensive approach to revealing the relationship between calf growth state and core gut microbes. However, the identification of beneficial gut bacteria and its internal mechanisms of shaping host phenotype differentiation remains unclear.

Results In this study, calves were divided into two clusters, cluster1 and cluster2, based on 29 phenotypic indicators using cluster analysis. Calves in cluster2 showed better growth performance, including higher body weight (BW), average daily gain (ADG), and dry matter intake (DMI), as well as better serum indicators with a high level of total superoxide dismutase (T-SOD), interleukin-6 (IL-6), and insulin-like growth factor-1 (IGF-1) compared to those in cluster1. Multi-omics was used to detect microbial features among calves in different phenotypic clusters. Distinct differences were observed between the two clustered gut microbiomes, including microbial diversity and composition. The close relationships between growth performance, blood metabolites, and microbiome were also confirmed. In cluster2, *Bifidobacterium* members were the dominant contributors to microbial metabolic functions with a higher abundance. Furthermore, pathways involved in carbohydrate degradation, glycolysis, and biosynthesis of propionate and proteins were active, while methane production was inhibited. In addition, the diversity and richness of hindgut resistome in cluster2 were lower than those in cluster1. The isolation and culture of *Bifidobacterium* strain, as well as the mice experiment, indicated that *B. longum 1109* from calf feces in cluster2 could promote the growth of young hosts, enhance their blood immunity and antioxidation, and improve the development of hindgut.

Conclusions In summary, cluster analysis has proved to be a feasible and reliable approach for identifying phenotypic subgroups of calves, prompting further exploration of host-microbiome interactions. *Bifidobacterium* as a core microbe in the hindgut of calves may play a crucial probiotic role in host phenotypic differentiation. This study enhances our comprehension of how gut core microbe shapes the host phenotype and provides new insights

†Yimin Zhuang, Duo Gao and Wen Jiang contributed equally to the study.

*Correspondence:
Zhijun Cao
caozhijun@cau.edu.cn
Full list of author information is available at the end of the article

into the manipulation of beneficial gut colonizers to improve the growth performance and productivity of young ruminants.

Keywords Calf, Phenotypic clustering, Core microbe, Multi-omics

Introduction

Ruminants, particularly cows, are important livestock animals widely raised around the world for their high-quality and protein-rich milk. Recent evidence suggests that the growth performance and health of young ruminants are directly regulated by the gut microbiome, which profoundly impacts their productivity in adulthood [1–3]. This emphasizes the importance of calf-associated microbes in the dairy production system. The gut microbiome is highly efficient at utilizing nutrients, particularly in its ability to decompose plant substances such as cellulose and hemicellulose, which are indigested by the host. This process results in the production of volatile fatty acids (VFA) and microbial proteins that can be reabsorbed by the host. In addition, the gut microbiome is intimately involved in host physiology, including gut epithelial development [4], mastitis [5], metabolic homeostasis [6], and immunity [7]. Therefore, a thorough investigation of the calf gut microbiome is beneficial for developing more rational diet regimes and improving existing feeding strategies to further enhance dairy cow production.

Previous studies have explored the relationship between different ruminant phenotypes and gut microbiota. Calves are typically grouped based on subjective evaluations of one or more indicators, such as growth rate [8], methane production [9], milk yield, and serum indexes (e.g., β-hydroxybutyrate (BHBA) [10] and total antioxidant capacity (T-AOC)) [11]. Although the relationship between gut microbiota and ruminant phenotype has been studied, it is crucial to note that accurate grouping becomes increasingly challenging with the addition of more factors. In such cases, subjective judgment used for grouping is likely to introduce bias, which may negatively affect the reliability and generalizability of the study results. Currently, unsupervised cluster analysis stands as the most appropriate method. While some studies have shown that there are physiological differences among cows in different clustering groups [12], it is still unclear how the phenotype of calves in these groups relates to their gut microbiome. Is there a significant difference in the gut microbiota of calves from different phenotypic clusters? Can gut core microbes drive phenotypic differentiation? Which microbial metabolic functions could be affected during this process?

In this study, to answer the questions above, we performed cluster analysis on 32 calves based on 29 phenotypic indicators and characterized the top influencing factors. In addition, multi-omics technology (including 16 s rRNA gene sequencing, metagenomics, and metabolomics) was used to classify the core microbes that dominate the calf phenotype. The related metabolic pathways regulated by the core microbes were also identified. The study showed that cluster analysis is useful in examining the connection between phenotype and gut microbiota in calves. It also highlighted the importance of core microbes in phenotypic differentiation.

Result

The identification of calf subgroups with different growth performance by phenotypic clustering

A total of 29 apparent indexes were included as a set of data variables in the phenotypic clustering, including colostrum feeding (CL), 70-day-old body weight (BW), average daily gain (ADG), withers height (WH), body length (BL), heart girth (HG), cannon bone circumference (CBC), liquid dry matter intake (LDMI, DMI of whole milk and milk replacer), concentrate DMI (CDMI, DMI of starter), forage DMI (FDMI, DMI of forage), solid DMI (SDMI, DMI of starter and forage), DMI (total DMI), concentrate/forage (C/F), feed conversion ratio (FCR), diarrhea score (DS), and serum indicators (GLU, total protein (TP), albumin (ALB), UREA, total superoxide dismutase (T-SOD), T-AOC, glutathione peroxidase (GSH-PX), malonaldehyde (MDA), non-esterified fatty acids (NEFA), interleukin-1β (IL-1β), interleukin-6 (IL-6), tumor necrosis factor-α (TNF-α), insulin-like growth factor-1 (IGF-1), and BHBA).

Based on the average silhouette width from k-means clustering analysis (Fig. 1A), dividing the 32 calves into 2 clusters (Fig. 1B) yielded the highest clustering robustness. Following the clustering procedure, cluster1 encompassed a total of 18 calves, whereas cluster2 comprised the remaining 14 calves. The descriptive statistics and comparative analysis of phenotypic indicators for cluster1 and cluster2 were displayed in Table S1 and S2 respectively. Specifically, BW and ADG were the critical variables affecting the clustering results, followed by FCR, CL, IL-6 and IGF-1 (Fig. 1C). Compared to cluster1, the calves in the cluster2 showed a better growth performance with a higher BW, WH, ADG, BL, HG, LDMI, CDMI, FDMI, SDMI, DMI ($P < 0.05$) and a lower FCR ($P < 0.05$). Moreover, concentrations of several serum

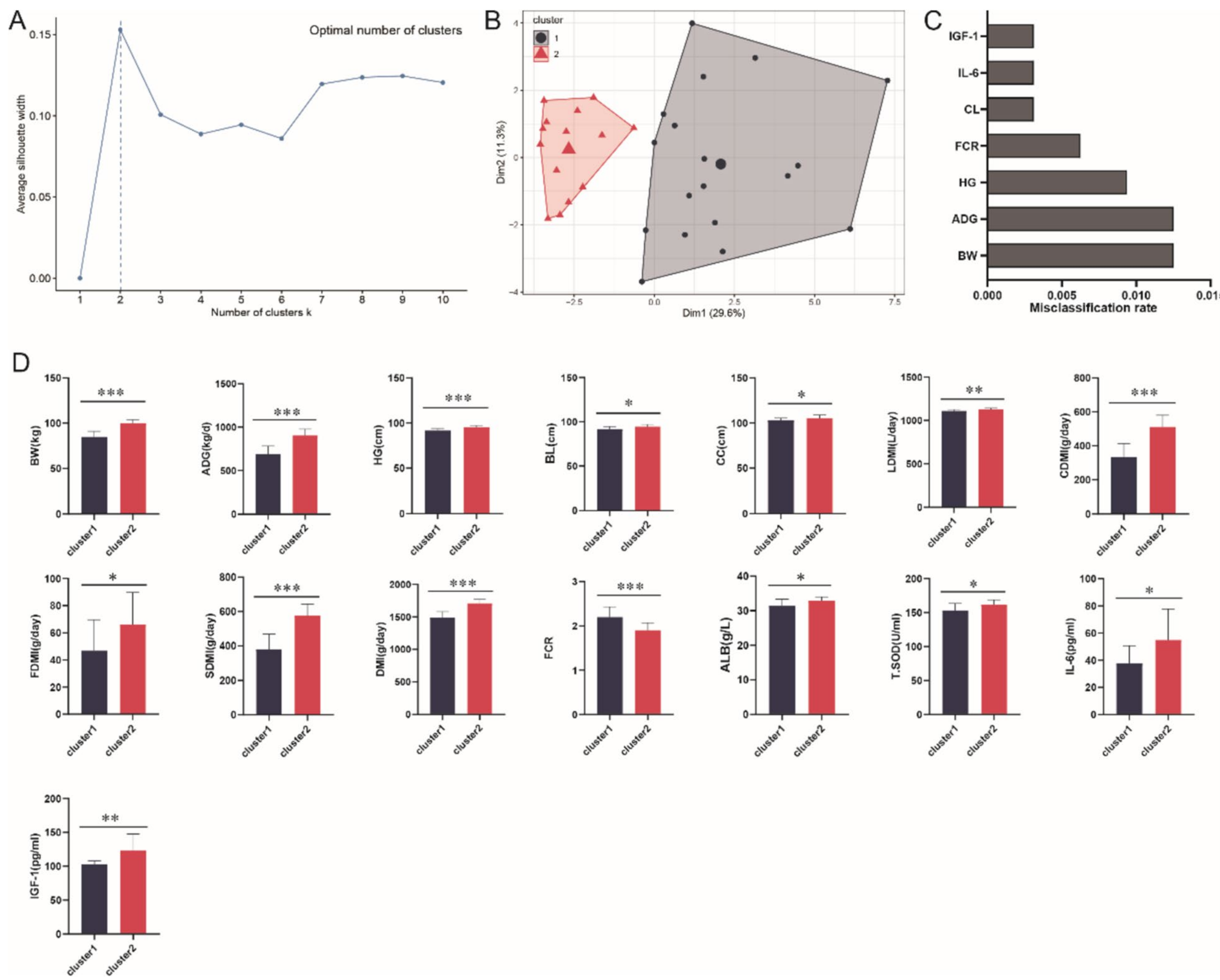

Fig. 1 Phenotypic clustering results of 32 calves with apparent factors. **A** Silhouette coefficient to determine optimal number of clusters.**B** Visualising the results of k-means clustering. **C** Importance of each apparent factor in the cluster analysis. (Displaying the top seven apparent factors in order of importance). **D** The indicators with significant difference in the cluster1 and cluster2. (*$P<0.05$, ** $P<0.01$, *** $P<0.001$).

indicators, including ALB, T-SOD, IL-6, and IGF-1, were significantly higher in cluster2 than in cluster1 ($P<0.05$) (Fig. 1D).

The distinct difference in the microbial community of calves between the two clusters

To further deepen our understanding of the relationship between phenotypic differentiation and gut microbiota, the microbial profiles of these two clusters were characterized using 16 s rRNA gene sequencing. As shown in Fig. 2A–C. The microbial diversity and structure were distinct between these two clusters. Specifically, the Chao1 (Fig. 2A) and Shannon index (Fig. 2B) were significantly higher in cluster1 than in cluster2 ($P<0.05$). The principal coordinate analysis (PCoA) plots based on Bray–Curtis with ANOSIM analysis also showed a remarkable distance in the two clusters ($P<0.001$, $R=0.728$) (Fig. 2C).

(See figure on next page.)

Fig. 2 The differences in gut microbiota diversity and structure between cluster1 and cluster2 calves. **A** The Chao1 index of gut microbiota between cluster1 and cluster2 calves. **B** The Shannon index of gut microbiota between cluster1 and cluster2 calves. **C** The principal coordinate analysis (PCoA) of the hindgut microbiota in the two differential clusters with ANOSIM analysis. **D** Composition of the gut microbiota at the phylum level. **E** Composition of the gut microbiota at the genus level. **F** the identification of signature genera in the cluster1 and cluster2 using linear discriminant analysis (LDA) effect size (LEfSe) analysis.**G** Spearman's correlation of gut microbiota and apparent factors.

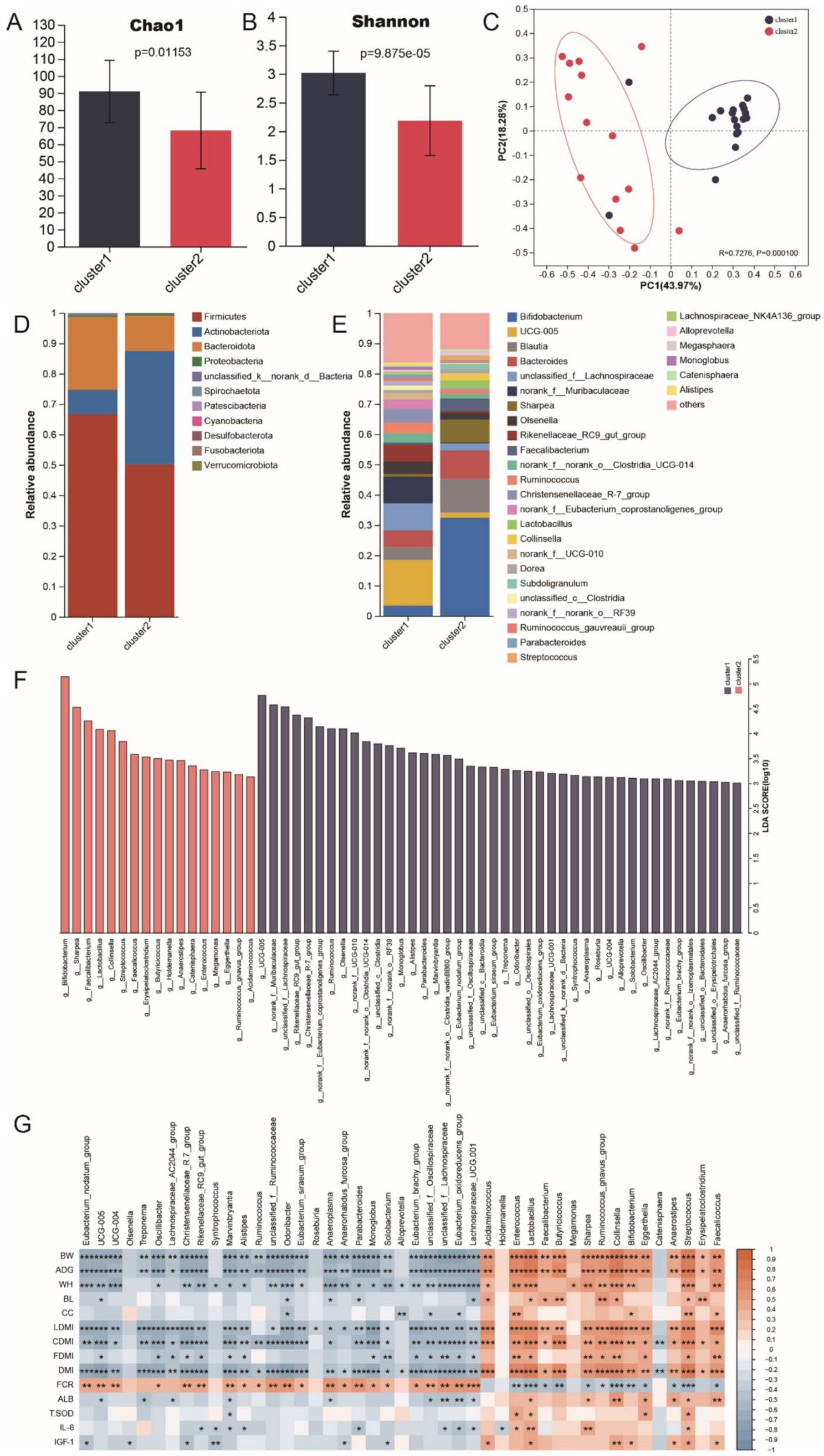

Fig. 2 (See legend on previous page.)

At the phylum level, Firmicutes, Bacteroidetes, and Actinobacteriota were the dominant bacteria in both clusters (relative abundances > 5% in both groups) (Fig. 2D). Firmicutes and Bacteroidetes were higher in abundance in the cluster1 than that in the cluster2, while Actinobacteriota showed an opposite trend ($P < 0.05$) (Fig. S1A). At the genus level, *UCG-005*, *unclassified_f_Lachnospiraceae,* and *norank_f_Muribaculaceae* were the three most abundant genera in cluster1 (Fig. 2E) with their abundances being significantly higher than those in cluster 2 ($P < 0.05$) (Fig. S1B). In the cluster2, *Bifidobacterium* was the most abundant genus followed by *Blautia*, *Bacteroides,* and *Sharpea* (Fig. 2E). Moreover, the genera of *Bifidobacterium*, *Sharpea,* and *Faecalibacterium* showed a higher abundance in the cluster2 compared with the cluster1 ($P < 0.05$) (Fig. S1B). Then, linear discriminant analysis (LDA) effect size (LEfSe) was performed to identify the signature genera in the two clusters respectively ($P < 0.05$ and LDA > 3) (Fig. 2F). *UCG-005*, *unclassified_f_Lachnospiraceae*, *norank_f_Muribaculaceae*, *Rikenellaceae_RC9_gut_group*, *Olsenella*, and *Ruminococcus* were identified as signatures in the cluster1. In the cluster2, fewer signature microbes were observed including well-known functional bacteria *Bifidobacterium*, *Sharpea*, *Faecalibacterium*, *Lactobacillus*, and *Streptococcus*. Moreover, a Spearman analysis between these microbes identified by LEfSe and apparent factors was conducted to detect the interaction between microbiota and phenotypes ($P < 0.05$ and $R > 0.5$). As expected, general correlations were observed (Fig. 2G). Specifically, the microbes in the cluster1 were negatively correlated with BW, ADG, BH, LDMI, CDMI, DMI, ALB, IL-6, and IGF-1 and positively correlated with FCR. While the positive or negative correlations between the microbes in the culster2 and these factors had the opposite results from cluster1. We also used Procrustes Analysis to evaluate the consistency between the phenotypic data set and the calf gut microbiological data set (Fig. S2). The results showed a trend of significant consistency between these two data sets ($P = 0.084$).

Co-occurrence network of gut microbial interactions in the calves of cluster1 and cluster2

The co-occurrence networks of gut microbiota in calves for the two clusters were analyzed to determine the probability of interactions between bacteria ($P < 0.05$ and $R > 0.5$). According to the global network graph, compared with cluster2, the network of cluster1 showed a more complex interaction with more bacteria nodes and correlated edges (Fig. 3A, C). Furthermore, using the MCODE plugin [13] in Cytoscape with programmed parameters (degree cutoff: 2; K-Core: 2; and max depth: 100), the core networks of the two clusters were identified separately. We observed the signature *UCG-005* was the hub node in the cluster1 core network (Fig. 3B). Similarly, *Blautia* and *Bifidobacterium* as hub nodes were identified in the cluster2 core network (Fig. 3D).

Enrichment of Bifidobacterium members in the gut of calves with good phenotype

In the next step, metagenome was used to further annotate the bacteria at the species level and determine the dominant functional pathways in the gut microbiome of calves of different phenotypic clusters. Consistent with the 16 s rRNA gene sequencing results, the PCoA plot at the species level showed a significant distance between two clusters ($P = 0.002$, $R = 0.732$) (Fig. S3). Several *Bifidobacterium* members were significantly more abundant in the cluster2 compared with the cluster1 including *Bifidobacterium pseudocatenulatum*, *Bifidobacterium longum*, and *unclassified_g_Bifdobacterium* ($P < 0.05$). In contrast, *Lachnospiraceae bacterium*, *Oscillospiraceae bacterium*, *Clostridia bacterium*, *Olsenella sp*., and *Ruminococcus sp*. showed higher abundance in the cluster1 ($P < 0.05$) (Fig. 4A). Then, Hungate1000 collection [14], a database of bacterial and archaeal species isolated and cultured from the gut of a variety of ruminants, was used to further deepen our understandings of microbial taxa identification at a strain-level in this study. As shown in Fig. 4B, B. *longum AGR2137*, *B. adolescentis DSM 20087*, *B. breve RP2*, *B. merycicum DSM 6492*, and *B. ruminantium DSM 6489* were the dominant strains in the cluster2, which favored starch utilization and production of acetate and lactate. In addition, *Blautia* members, including *B. sp. SF-50* and *B. wexlerae AGR2146,* and *Streptococcus* members, including *S. equinus AR3*, *S. gallolyticus LMG 15572*, *VTM1R29*, *VTM2R47*, *VTM3R24*, and *VTM3R42* were abundant in the cluster2 with the ability to utilize starch and protein and produce lactate. Notably, we observed that one methanogenic strain (*Methanobrevibacter wolinii SH*) was enriched in the cluster1.

Characteristics of metabolic functions of gut microbiome in the calves of two clusters

Metagenomic functional analysis showed the distinct features between the cluster1 and cluster2. At the KEGG level2, we observed a significant difference in metabolic functions related to amino acid, energy, vitamins, and cofactors between the two clusters ($P < 0.05$) (Fig. S4). In terms of metabolic functions, the results of LEfSe indicated the KEGG pathways of pyruvate metabolism, methane metabolism, butanoate metabolism, alanine, aspartate, and glutamate metabolism, glycerolipid metabolism, and linoleic acid metabolism showed higher abundance in the calves of cluster1. For the cluster2, the pathways of amino acid metabolism were

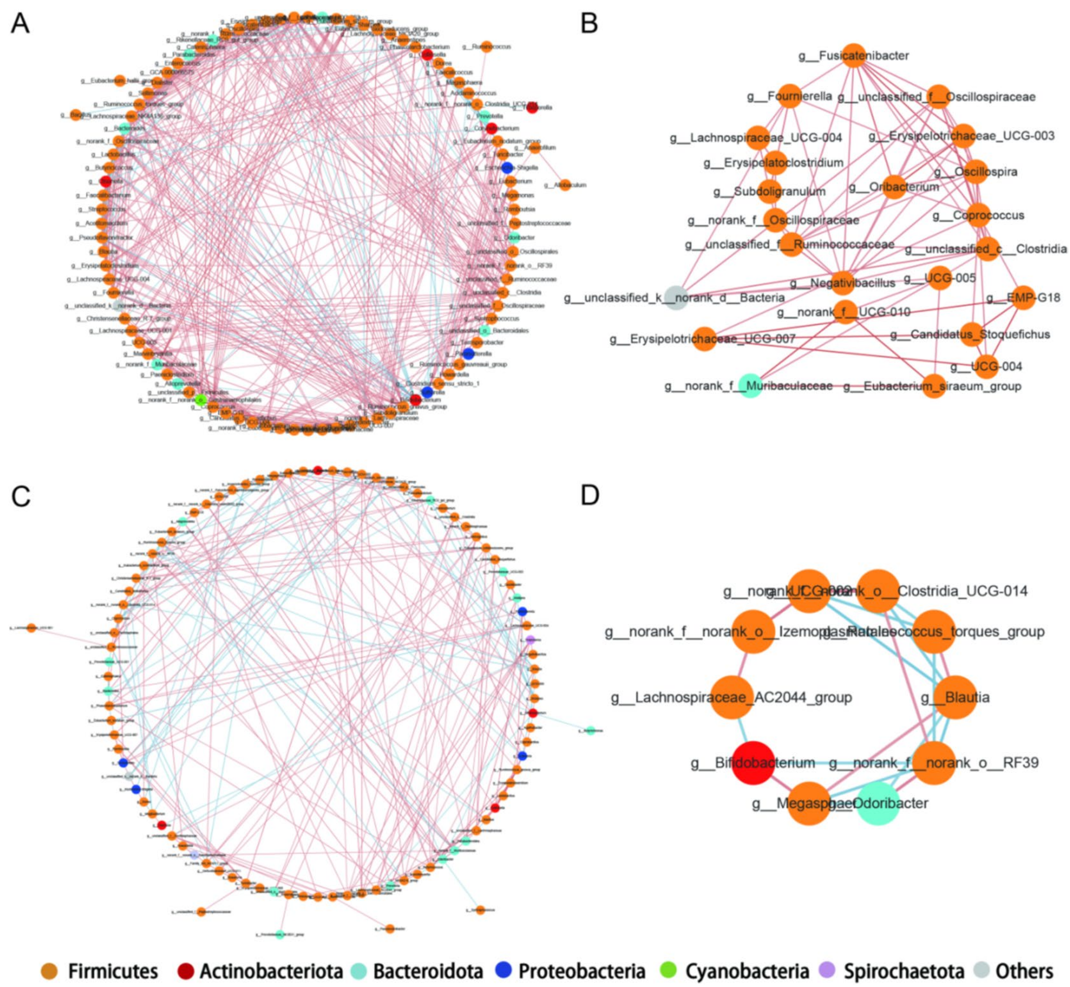

Fig. 3 Co-occurrence networks of gut microbiota in the cluster1 and cluster2 calves. **A** Cluster1 gut microbial co-occurrence network. **B** Cluster1 gut microbial core network. **C** Cluster2 gut microbial co-occurrence network. **D** Cluster2 gut microbial core network. The color of connection lines between two nodes represents a positive (red) or a negative (blue) correlation.

active including cysteine and methionine metabolism, valine, leucine, and isoleucine biosynthesis, phenylalanine, tyrosine, and tryptophan biosynthesis, glutathione metabolism, and arginine and proline metabolism. In addition, the pathways of starch and sucrose metabolism, galactose metabolism, and propanoate metabolism had a similar dominant trend in the cluster2 (Fig. 5A). We further track the microbial hosts of eight major metabolic functions. In the cluster1, *Oscillospiraceae bacterium*, *Lachnospiraceae bacterium*, *Clostridia bacterium* and *Bacteroidales bacterium* were the main microbial host of metabolic functions. While in the cluster2, *Bifidobacterium longum*, *Bifidobacterium pseudocatenulatum*, *Sharpea azabuensis,* and *unclassified_g_Bifdobacterium* were the dominant species, highlighting its important role in the metabolic functions (Fig. 5B).

Using the KEGG Mapper, the dominant metabolic pathways enriched by high-abundance enzymes in the calf gut microbiome of two clusters were visualized (Fig. 5C). In the cluster1, starch and sucrose metabolism, glycolysis, amino acid metabolism and biosynthesis of acetate and propanoate with enriched enzymes of *EC 2.7.1.211*, *EC 2.7.1.4*, *EC 3.2.1.68*, *EC 3.2.1.141*, *EC 2.7.1.205*, *EC 1.2. 1.9*, *EC 4.2.1.11*, *EC 1.3.3.6*, *EC 1.1.85*, and *EC 2.8.3.18*. Conversely, methane metabolism was enriched by the enzymes of *EC 1.2.7.4*, *EC 1.2.7.12*, *EC 1.5.98.1*, *EC 1.5.98.2*, *EC 2.1.1.86*, and *EC 2.8.4.1* in the cluster2.

Next, we focused on carbohydrate-active enzymes (CAZyme) abundance in the two clusters. In both clusters, glycoside hydrolases (GHs) had the highest abundance among the seven CAZyme classes followed by glycosyl transferases and carbohydrate esterases (Fig. S5A). In addition, we also observed the remarkable difference of GHs composition based on the PCoA plots with ANOSIM analysis ($P=0.002$, $R=0.568$) (Fig. S5B).

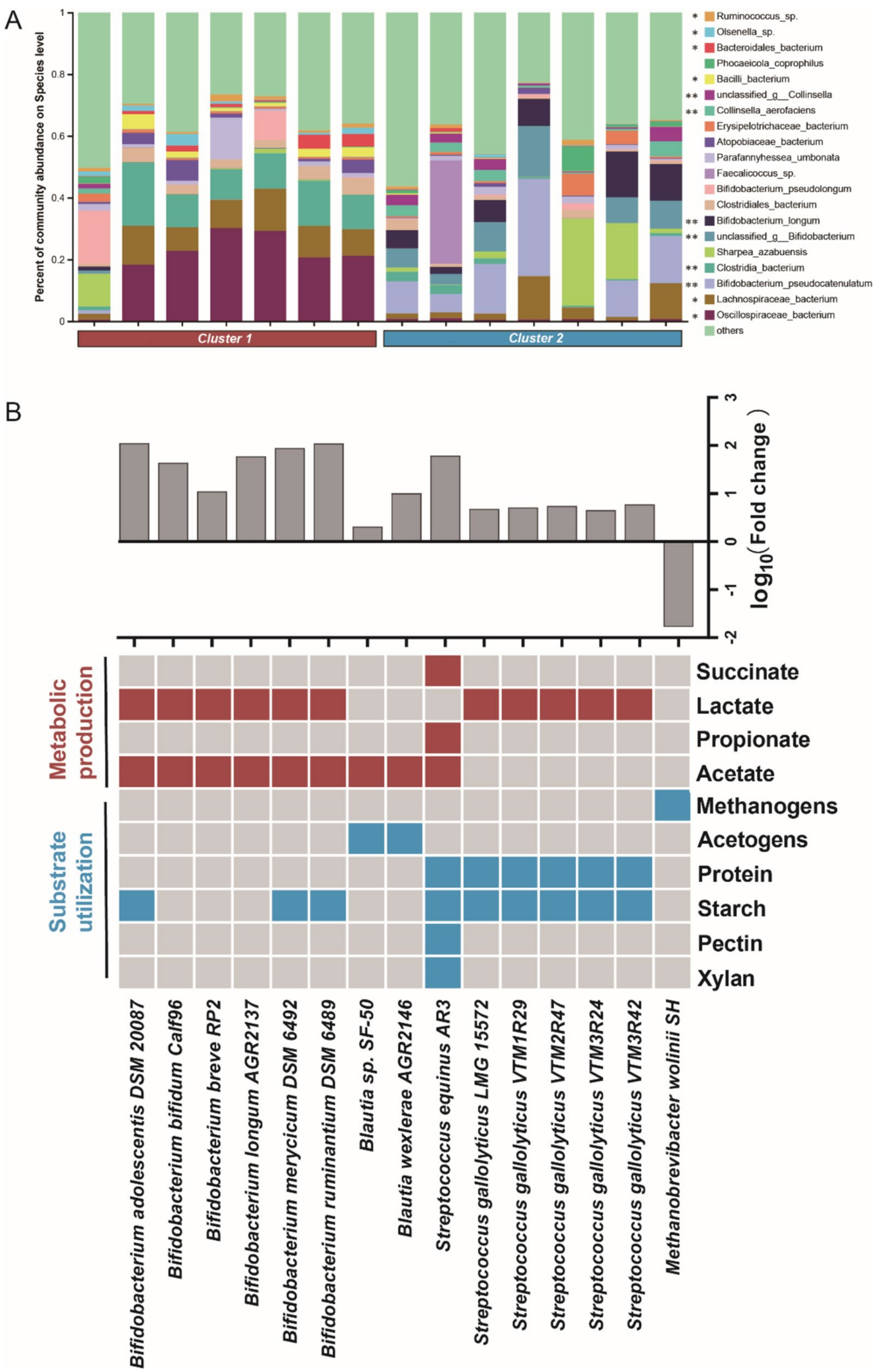

Fig. 4 The *Bifidobacterium*-dominated microbiome contributed to phenotypes of calves. **A** The composition of gut microbiota at the species level in the cluster1and cluster2. **B** The identification of cultured strains in the Hungate1000 collection.

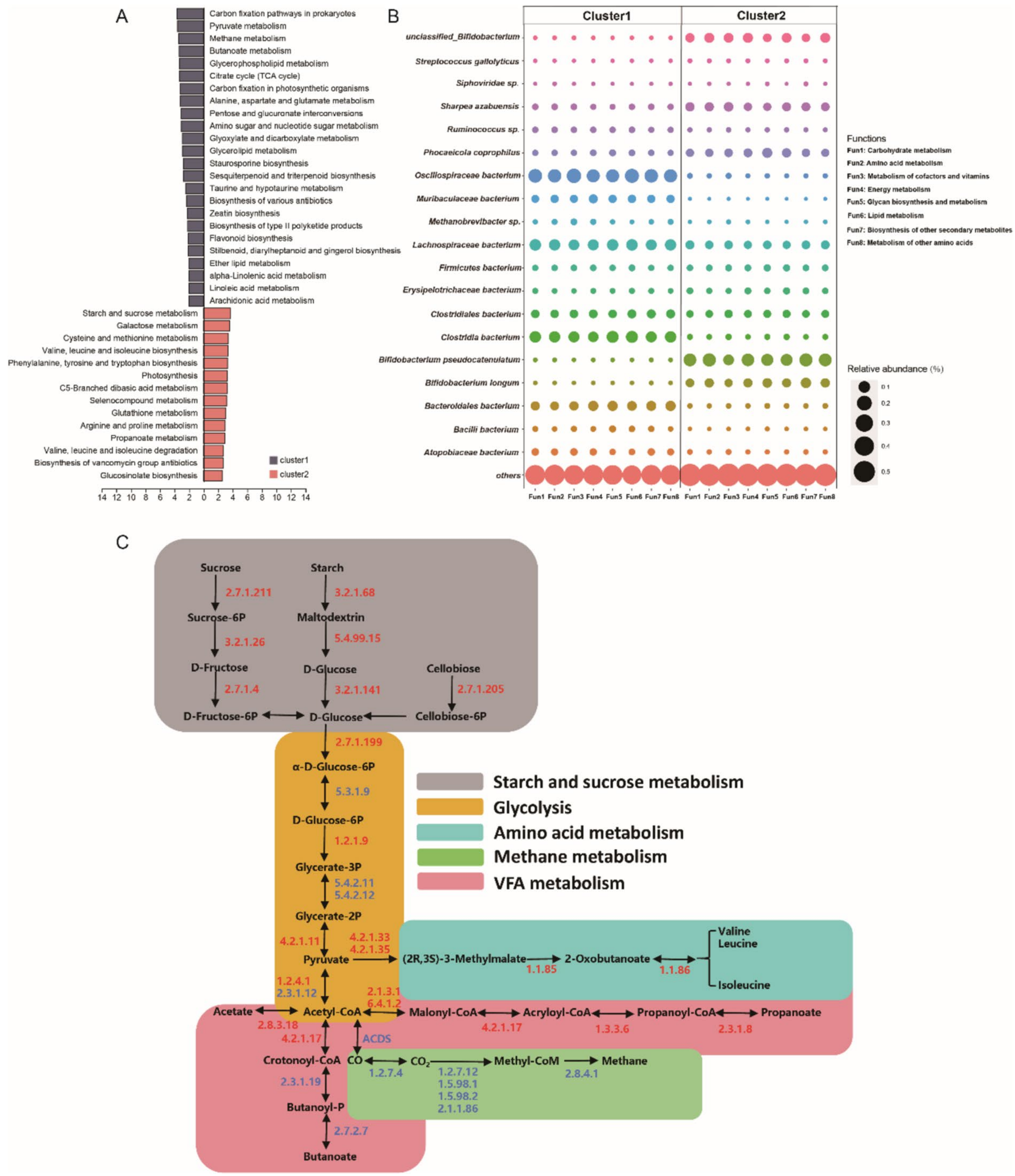

Fig. 5 The difference of KEGG metabolic function attached to gut microbiome between the cluster1 and cluster2. **A** Significantly different KEGG pathways related to metabolism of fecal microbiota in the cluster1 and cluster2. **B** Bubble plots depicting the difference of microbial hosts of metabolic functions at the species level. **C** Integration of significantly different metabolic pathways involved in starch and sucrose metabolism, glycolysis, amino acid metabolism, methane metabolism and VFA metabolism.

Hence, we further detected the abundance of GH members between the clusters. The abundance of four dominant GH members, including GH20, GH32, GH42, and GH8, was higher in cluster2 than in cluster1 ($P<0.05$) (Fig. S5C).

Finally, a distinct difference in gut resistome structure was observed between the two clustered groups

($P = 0.005$, $R = 0.576$) (Fig. 6A). Compared with cluster2, the gut microbiome of calves in cluster1 might carry more pressure from antibiotics resistance genes (ARG) including higher ARG richness ($P = 0.004$) (Fig. 6B) and diversity ($P = 0.011$) (Fig. 6C). In terms of antibiotic class, Multidrug, MLS, Glycopeptide, Tetracycline, and Peptitie were the top 5 dominant antibiotic resistance classes across the two clusters (Fig. 6D). Among the main ARGs, the ARGs of *macB*, *mtrA*, *lmrD*, *baaS*, *patB*, *efrB*, and *kdpE* were enriched in the cluster2, while *oleC*, *Sris_parY_AMU*, *vanRF*, *rpoB2*, *optrA*, *evgS*, *bacA*, and *Saur_mupA_MUP* were abundant in the cluster1 ($P < 0.05$) (Fig. 6E).

Significant differences in the metabolic profiles between the cluster1 and cluster2 calves

The untargeted metabolomics analysis of gut microbiome in the calves of cluster1 and cluster2 was performed. The partial least squares-discriminant analysis (PLS-DA) showed distinct metabolic profiles of gut microbiome between the two clusters (Fig. 7A). A total of 2275 gut metabolites were quantified, among which 66 metabolites were higher in the cluster2 and 227 were abundant in the cluster1 ($P < 0.05$). Considering the close interaction between the microbiome and the host, MetOrigin analysis [15] was conducted to track the origin of these differential metabolites. The results showed that 19 metabolites originated from the host, 44 metabolites were derived from the microbiota, and 15 metabolites

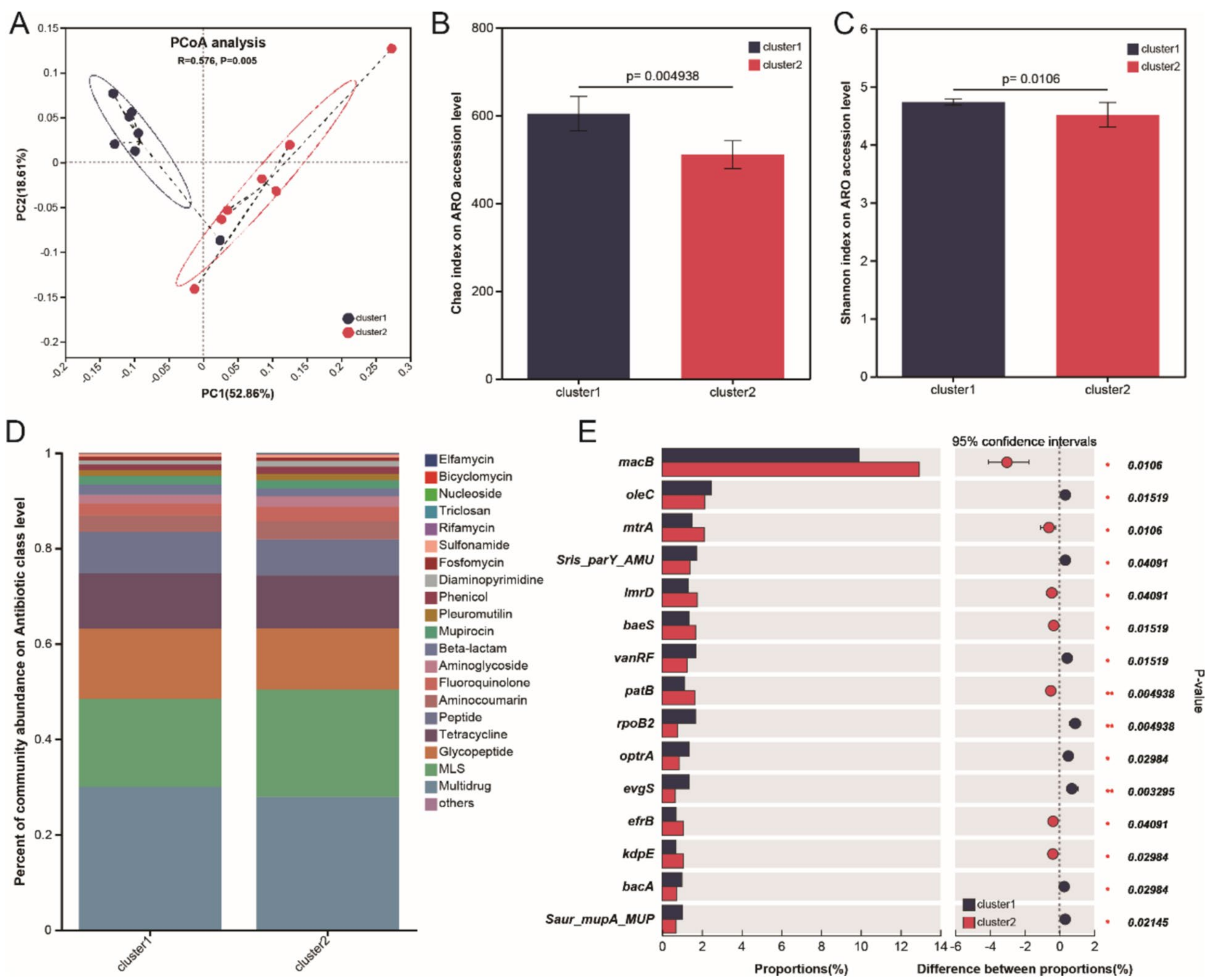

Fig. 6 Differences in the hindgut resistome in cluster1 and cluster2. **A** The principal coordinate analysis (PCoA) of the hindgut resistome in the two clusters with ANOSIM analysis. **B** Chao1 index of resistome between cluster1 and cluster2 calves. **C** The Shannon index of resistome between cluster1 and cluster2 calves. **D** The resistome composition of drug classes between the two clusters. **E** The comparison of main antimicrobial resistance genes (ARGs) in the two clusters.

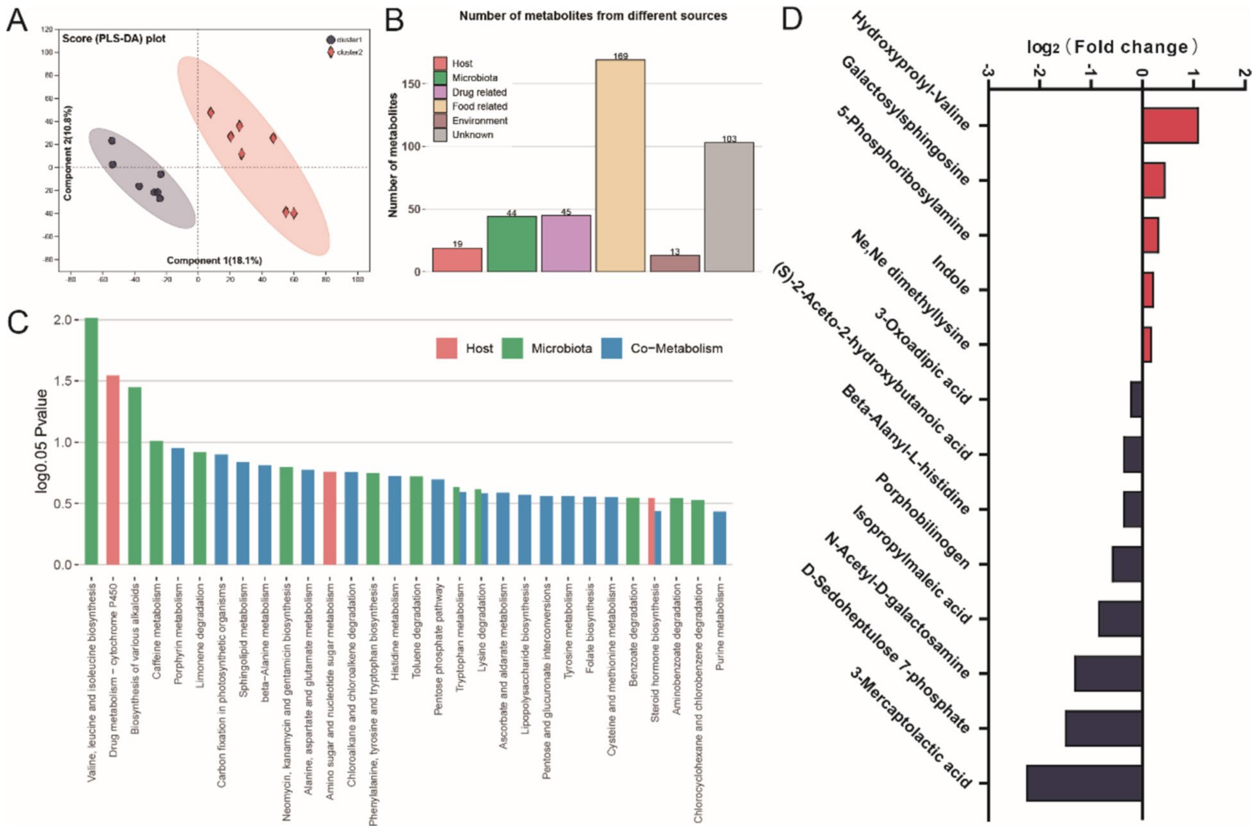

Fig. 7 The fecal metabolic profile of the cluster1and cluster2. **A** Partial least squares-discriminant analysis (PLS-DA) of the fecal metabolome between the cluster1and cluster2 calves. **B** The identification of fecal metabolites from different sources. **C** Metabolic pathway enrichment analysis according to different categories of metabolites belonging to the different sources. **D** The up-regulated metabolites enriched and the down-regulated metabolites enriched in the metabolic pathways.

were shared by the two (Fig. S6); the remaining metabolites were from other sources (drugs, food, environment, and unknown) (Fig. 7B). The enrichment analysis of these metabolites was performed to identify the remarkable metabolic pathways. Consistent with the results of microbial functions, the metabolism related to amino acid was active including valine, leucine and isoleucine biosynthesis, beta−alanine metabolism, alanine, aspartate, and glutamate metabolism (Fig. 7C). These metabolic pathways were enriched by the upregulated signature metabolites hydroxypropyl-valine, galactosylsphingosine, 5-phosphoribosylamine, indole, Ne,Ne dimethyllysine and downregulated metabolites 3-oxoadipic acid, (S)−2-Aceto-2-hydroxybutanoic acid, beta-Alanyl-L-histidine, porphobilinogen, isopropylmaleic acid, N-Acetyl-D-galactosamine, D-Sedoheptulose 7-phosphate and 3-mercaptolactic acid (Fig. 7D).

B. longum administration improved growth phenotype and hindgut development of young mice

Although the above results indicated that the *Bifidobacterium*-dominated microbiome might be an important driving force for improving the phenotype of calves, considering the complex interactions between microbial communities in feces, it is necessary to further verify the general probiotic effect of *Bifidobacterium* to host from the feces of cluster2 calves at the level of a single strain. We successfully isolated a strain of *B. longum* (named *B. longum 1109*) from the feces of these calves through the technique of bacterial isolation and culture, and fed it to mice to observe their phenotypic changes (Fig. 8A). According to the results, from the fourth day to the end of the experiment, the BW and ADG of treatment (TRT) mice (*B. longum 1109* administration) were significantly higher than the control (CON) mice (Phosphate Buffered Saline (PBS) administration) ($P < 0.05$) (Fig. 8B–D). Although there was no significant difference in colon length between the two groups of mice (Fig. S7), we also observed their distinct difference in the morphology of the colon tissue. The TRT mice showed a more complete and compact colonic epithelial structure and a deeper crypt, suggesting a higher degree of colonic development ($P < 0.05$) (Fig. 8E, F). In addition, the results of serum metabolites indicated that *B. longum 1109* administration could reduce the risk of inflammation and enhance the host's immunity and antioxidant capacity, reflected in the lower concentration of IL-1β, IL-6, and MDA, and higher concentration of IgA, IgM, IgG, Glutathione (GSH), and GSH-PX ($P<0.05$) (Fig. 8G). Notably, the growth factor of IGF-1 in the mice of the TRT group was also higher in concentration, which was consistent with the calf results ($P<0.05$) (Fig. 8G).

Discussion

The healthy and efficient development of young ruminants can determine their lifelong consequences and is closely associated with the gut microbiome. To effectively identify gut core functional bacteria and clarify their potential beneficial and growth-promoting effects, it is necessary to have a deep understanding of the differences and characteristics of gut microbial structure and metabolic functions among calf populations with different phenotypes. This study utilized the k-means clustering method to reduce and cluster multi-factor high-dimensional apparent data sets. As a result, two calf populations with significant phenotypic differences were accurately identified. Multi-omics techniques were employed to demonstrate the crucial role of the gut microbiome in phenotypic differentiation.

Cluster analysis is a method that can combine several factors (e.g., growth rate, health indicators, and body dimensions) to provide a more comprehensive assessment of overall calf performance. The comprehensive nature of the calf classification obtained from clustering renders it more accurate and reliable. Furthermore, cluster analysis may identify potential associations that have been overlooked in single-factor studies. For instance, some calves with moderate growth rates may be classified as "good" calves due to other advantages, such as superior immunity or healthier gut microbiology. Indeed, numerous relationships within biological systems are intricate and may be influenced by the interaction among multiple factors. Cluster analysis can assist in the elucidation of these intricate relationships, particularly in the relationship between gut microbes and calf phenotype. Due to the potential association of certain gut microbes with multiple calf phenotypic traits, the detection of these relationships may be challenging in single-factor studies. Consequently, we proceeded to investigate the gut microbial differences between the various calf groups, based on the clustering results, and to ascertain the impact of these differences on calf phenotypic traits. In practice, cluster analyses that combine several factors can help farmers in the identification and management of calves with differing performance characteristics. In this study, the selection of phenotypic clustering index included two categories: growth performance indexes and blood metabolism indexes. As we know, growth performance is the most intuitive index to evaluate the development efficiency of calves, which is often closely related to the metabolic state of the host. For instance, calves with better growth performance also had higher concentrations of IGF-1 in the blood [16–18]. Therefore, some iconic blood metabolites were also covered in the cluster analysis. The results of the clustering analysis showed that several serum indexes, including ALB, T-SOD, IL-6, and IGF-1, contributed significantly to the classification of clusters, in addition to the primary growth performance indicators. This suggests a close relationship and synchronicity between host metabolism and its growth state. IGF-1 is recognized as a critical growth-promoting factor in children and young mammals. It plays an important regulatory role in host development and endocrine metabolism [19, 20]. A recent study reported that calves fed diets with higher starch content experience a simultaneous increase in plasma IGF-1 concentration [21]. T-SOD is an antioxidant factor synthesized independently by the host that can improve cellular immunity and relieve oxidative stress [22, 23]. A study has shown that supplementing alkaline mineral compound water to calves with diarrhea effectively reduces the diarrhea rate and increases plasma antioxidant capacity and IGF-1 concentration [24]. The study found that calves in cluster2 exhibited better growth performance due to increased solid feed consumption and higher concentrations of growth and antioxidant factors in their serum. These factors appear to be intrinsic promoters of rapid calf development, which is consistent with previous research.

As anticipated, we also verified the distinct microbial profile between these two clusters. Clusters 2 showed signatures of more beneficial bacteria, such as *Bifidobacterium, Faecalibacterium*, *Lactobacillus*, and *Butyricicoccus*, which were positively correlated with growth

(See figure on next page.)

Fig. 8 Effects of *B. longum 1109* from cluster2 calves on growth performance and colonic development of mice. **A** Experimental design diagram. **B** Body condition images of mice in the two groups. **C** Body weight (BW) of mice in the CON and TRT group. **D** The average daily gain between the two groups. **E** Representative H&E staining (×20 magnification) of representative colonic sections from each group. **F** The crypt depth of colon between the two groups. **G** The comparison of blood indicators including biochemistry (TP, ALB and GLB), inflammatory (IL-1β, IL-6 and TNF-α), immunity (IgA, IgM and IgG), IGF-1 and antioxidant (T-SOD, GSH-PX, MDA, T-AOC and GSH).

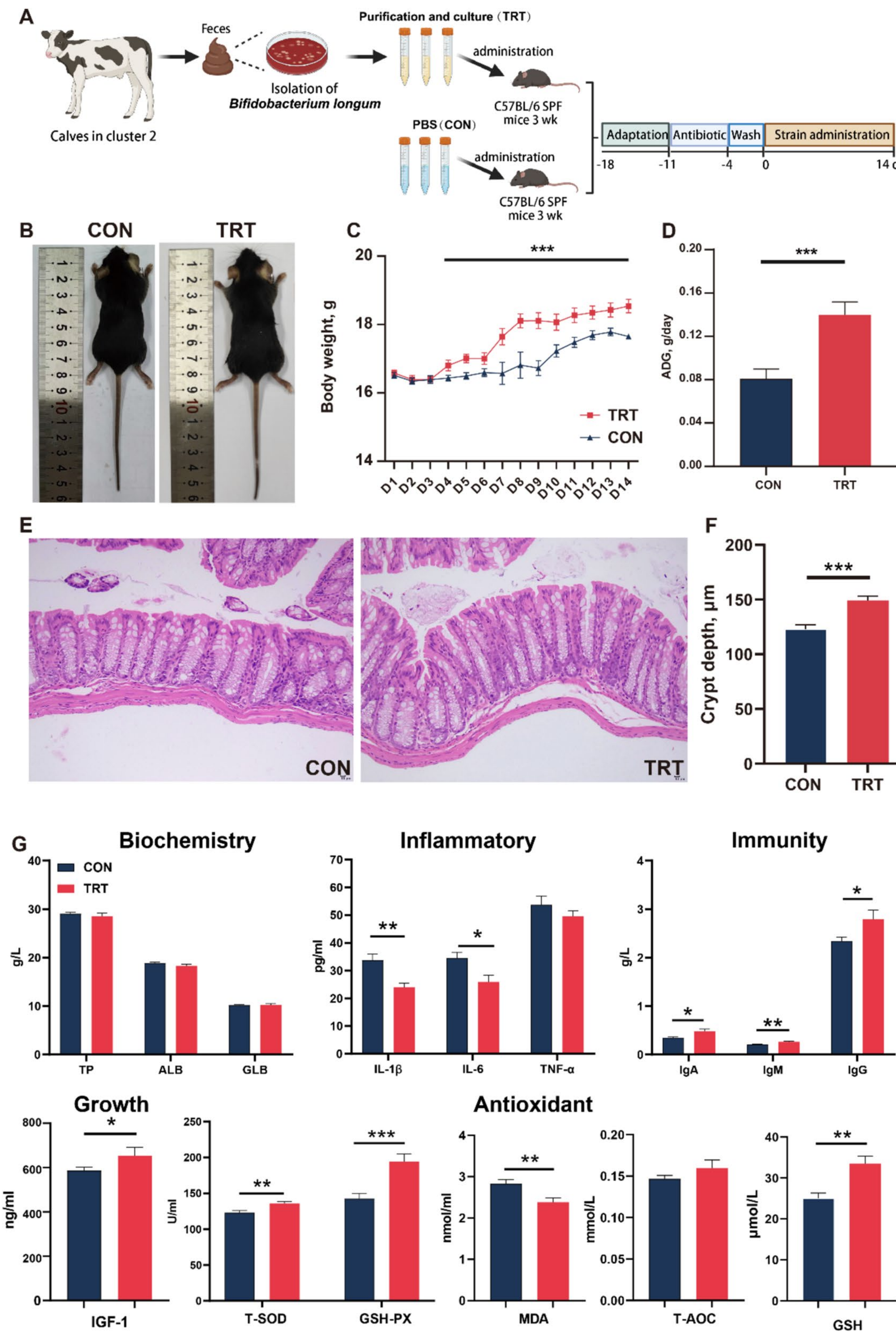

Fig. 8 (See legend on previous page.)

performance. *Bifidobacterium* is a core probiotic in the gut of both humans and animals. It has been extensively developed and commercialized [25]. The probiotic functions of different bifidobacterial species are diverse due to genetic diversity and variation [26]. These functions include efficient dietary fiber degradation, immune regulation [27], vitamin biosynthesis [28], and inhibition of host obesity [29] and senescence [30]. *Faecalibacterium* is considered a potential probiotic. Studies have shown that it is present in low levels in individuals with intestinal diseases and may serve as a candidate for disease biomarkers [31, 32]. In addition, *Faecalibacterium* can degrade plant cell walls and other bacterial metabolites and convert them into butyrate, as shown by in vitro and in vivo experiments [33, 34]. *Butyricicoccus* is a typical butyrate-producing bacterium. Co-culture with gut epithelial cells suggests that it has the ability to repair and maintain the integrity of the intestinal barrier [35]. *Lactobacillus* plays an indispensable role in maintaining animal gut health and is typically found in its colonization of the gastrointestinal tract of animals [36]. It is the most commonly used exogenous probiotic supplement. It can effectively inhibit the proliferation of pathogenic bacteria and maintain the microecological balance of the gut [37]. Our study highlights the significant contribution of microbes to shaping the excellent phenotype of cluster2 calves, as evidenced by the enrichment of beneficial bacteria in their gut. Notably, *Bifidobacterium* occupied the hub position in the core co-occurrence network of bacteria, suggesting it has a dominant niche in the gut microbial community [38]. The available evidence suggests that *Bifidobacterium* may be the core functional bacteria in the gut of cluster2 calves.

The metagenome technology was used to identify the enrichment of *Bifidobacterium* members in cluster2 at the species and strain level. The study found that *Bifidobacterium* members were the dominant bacteria responsible for executing metabolic functions in the gut of calves. This suggests that the dominant bacteria in the gut can drive the main metabolic directions of the whole gut microecology [39]. Specifically, the gut of cluster2 claves showed enrichment of enzymes related to the degradation of carbohydrates, such as starch, sucrose, and cellobiose. As is known, the adequate intake of feed, such as milk, concentrate, and forage provides the most direct carbon source for the metabolism and proliferation of gut microbiome in young ruminants [4, 40]. Most members of the genus *Bifidobacterium* are capable of utilizing monosaccharides, disaccharides, and oligosaccharides. Furthermore, species *B. longum* and *B. pseudocatenulatum* possess a range of genomes that encode enzymes capable of breaking down plant-based carbohydrates, indicating their potential to degrade such compounds [41, 42]. Our study found that high-abundance carbohydrate decomposers, mainly *Bifidobacterium*, colonized the gut of cluster2 calves to cope with increased feed intake. Therefore, it's not surprising that a higher abundance of degrading enzymes was identified in the cluster2. GHs are the largest and best studied category of Carbohydrate-active enzymes (CAZymes) that are responsible for the breakdown of carbohydrates [43]. In cluster2, we also observed the enrichment of four dominant GHs: GH20, GH32, GH42, and GH8. GH20 retains the glycoside hydrolase activity [44]. The GH32 family has enzymes that hydrolyze fructose and sucrose [45]. GH42 can efficiently degrade lactose, galacto-oligosaccharides, and galactans, suggesting that it may be involved in plant cell wall degradation [46]. Most enzymes in the GH8 family are endo-acting and are exclusively present in bacteria. They are highly efficient in decomposing cellulose, making them commonly referred to as 'cellulase family D' [47]. The activated CAZymes also make significant contributions to carbohydrate degradation in the gut of cluster2 calves. In the downstream metabolic pathways, the enzymes responsible for the biosynthesis of acetate and propanoate exhibited higher abundance in cluster2. Acetate is a short-chain fatty acid that is abundant in the gut. Several studies have shown that long-term acetate deficiency can cause abnormal lipid consumption and metabolism in the host [48] and accelerate the development of cognitive dysfunction in animals [49]. Propanoate produced by gut microbiota may reach the liver through blood circulation. In the liver, it undergoes gluconeogenesis and is converted into glucose for uptake and then utilized by host cells and organs [50]. As is known, VFA are the main metabolites produced by *Bifidobacterium* [51]. Therefore, the accumulation and diffusion of high-concentration VFA produced by *Bifidobacterium* in the gut of calves indirectly ensures their rapid development and health. The gut microbiome in cluster2 calves has a major metabolic trend of biosynthesizing amino acids, including valine, leucine, isoleucine, phenylalanine, tyrosine, and tryptophan. Amino acids are essential nutrients in animal development. Previous studies have reported that tryptophan supplementation can improve the antioxidant capacity of calves and alleviate their intestinal injury [52, 53]. Leucine and isoleucine were found to protect MAC-T cells from H_2O_2-induced oxidative stress by regulating pre-pantothenate metabolism [54]. The microbial functional pathway responsible for the biosynthesis of valine, leucine, and isoleucine was identified as the signature pathway in healthy calves following fecal bacteria transplantation [55]. This finding is consistent with our own results. Methane metabolism was found to be promoted in the gut of cluster1 calves. This is supported by the identification of the methanogenic strain *Methanobrevibacter wolinii SH* in cluster1. The previous study showed that reducing animal body fat through the production of methane [56], inhibiting methanogens could promote animal growth and production. Methane overproduction in the animal gut occurs because methanogens outcompete other nutrient-metabolizing bacteria for H_2 [9]. In cluster2, the more powerful *Bifidobacterium* compressed the proliferation space of methanogens, promoting the deposition of more nutrients in the host rather than their excretion as gas. This might be a reason for the better growth performance of calves in cluster2. Moreover, in the mice experiment, we found administration of *B. longum 1109* isolated from cluster2 calves could directly promote the host growth, hindgut development and improve host metabolism. In the previous studies, *Bifidobacterium* was proved to have a significant positive effect on the remission of colitis [57], nerve protection [58], and tumor resistance [59]. Our studies proved that the pro-growth effects on young animals might be another potential probiotic function of *Bifidobacterium*, which provided prospective guidance for the treatment of animal growth retardation and the improvement of production efficiency.

Conclusion

In summary, we used a cluster analysis method to accurately divide calves into two clusters according to their phenotypes. We further observed the close relationship between the distinct phenotypes of calves in different clusters and their gut microbiota. In the gut of cluster2 calves, core microbes dominated by *Bifidobacterium* occupied the main niche and were the main executor of microbial metabolic function. They improved host growth and development by promoting carbohydrate degradation, glycolysis, biosynthesis of propionate and proteins, and inhibiting methane production. Of note, the diversity and richness of hindgut resistome in cluster2 were lower than those in cluster1. The mice experiment proved the *B. longum 1109* isolated from the cluster2 calves showed the probiotic effects on the host phenotype and hindgut development. These results implicated that producers might be able to artificially screen and manipulate beneficial bacteria to colonize and proliferate in the gut, thereby enhancing the early development and future production potential of young ruminants.

Materials and methods

Animals and experimental design

A total of 32 healthy female Holstein dairy calves with similar birth weights (mean = 36.77 kg, SD = 1.43) were selected from the Gansu Tianmu Farm (Jin Chang, Gansu Province, P. R. China). The birth weights of the calves were recorded immediately after birth, and the calves were then assigned to individual hutches. The calves were reared together under the same environmental conditions, and the age difference between the calves was within 3 days. After birth, all the calves received 4 L of colostrum within 1 h from each individual dam. Following a serum TP test, only calves with a value of > 5.5 g/dL were included in the following experiment. All calves were fed according to the dietary regime of the farm from birth to 70 days of age. Specifically, the calves were fed whole milk from day 1 to day 22, with a 4-day transition to milk replacer and whole milk mixture beginning on day 22 and completely replaced with milk replacer powder after 25 days until day 70, during which time they were fed twice daily (0800 and 1600 h) according to Table S3. Additionally, the calves had unrestricted access to water, concentration, and forage from birth to 70 days of age (Table S4). All animals had the same diet and water. During the 70-day period, the feed intake (whole milk, concentrate, and forage) and diarrhea score of each calf were recorded every day. The body weight, WH, BL, HG, and CBC were measured using a calf weighing scale (Beijing Honneur Agriculture and Animal Husbandry Technology Co, Ltd, Beijing, P. R. China) and tape measure at specific time points: 0, 14, 28, 42, 56, and 70 days of age. Moreover, the fecal samples of each calf were collected with sterilized gloves before the morning feeding at 0600 h of 70 days of age and stored in the 5 mL frozen storage tubes. Similarly, blood was collected via jugular venipuncture once before the morning feeding (0700 h) of 70 days of age using 10 mL evacuated tubes. The collected blood was then subjected to centrifugation at 3000 × g for 10 min at 4 ℃ to obtain serum, which was stored in 1.5 mL microcentrifuge tubes. Both fecal and serum samples were rapidly frozen with liquid nitrogen and stored at − 80 °C for subsequent microbiological and serum analysis.

The health check consisted of three parts: fecal scoring, clinical examination of the respiratory system, and rectal temperature measurement. Fecal scores were recorded daily at 1000 h until day 70, following a 0 to 3 scoring system as outlined by Larson et al. [60]. The scores were as follows: 0 = firm, well-formed (not hard); 1 = soft, pudding-like; 2 = runny, pancake batter; and 3 = liquid, splatters, and pulpy orange juice. Data on fecal scores were collected by one independent trained observer. Diarrhea was defined as a score of 2 or 3. Although a few calves experienced transient and mild diarrhea in this study, we selected electrolytic solutions instead of antibiotics to treat them to avoid the effects of antibiotics on the gut microbiota of calves, which was also in line with the principle of farm treatment. Additionally, rectal temperature was checked weekly using a digital thermometer. The respiratory health of the calves was monitored daily before each feeding by visually inspecting nasal discharge and listening for breathing difficulties with auscultation by the farm veterinarian and a member of the research team. No respiratory diseases were observed throughout the study.

DNA extraction, PCR amplification, and 16 s rRNA gene processing

Dneasy PowerLyzer PowerSoil Kit (Qiagen, Inc., Germantown, MD, USA) was applied to extract the microbial DNA from the fecal samples of calves. Total DNA quality was checked with a Thermo NanoDrop 2000 UV microphotometer and 1% agarose gel electrophoresis. Primer pairs 338F (5′-ACTCCTACGG GAGGCA GCAG-3′)/806R (5′-GGACTACHVGGGTWTCTAAT-3′) were used to amplify the V3-V4 region of the bacterial 16S rRNA gene by an ABI GeneAmp® 9700 PCR thermocycler (ABI, CA, USA). Then the PCR reaction mixture was conducted and the product was collected from 2% agarose gel and purified using the AxyPrep DNA Gel Extraction Kit (Axygen Biosciences, Union City, CA, USA) using manufacturer's instructions and quantified using Quantus™ Fluorometer (Promega, USA). An Illumina Miseq PE250 platform (Illumina, San Diego, USA) was used to sequence amplicon libraries.

Raw FASTQ files were de-multiplexed by an in-house perl script, and then quality-filtered by fastp version 0.19.6 and merged by FLASH version 1.2.11 [61]. DADA2 was selected to de-noise the optimized sequences. Then taxonomic assignment of amplicon sequence variants (ASVs) was conducted by applying the Naive Bayes consensus taxonomy classifier implemented in Qiime2 and the SILVA 16S rRNA database (v138), and then adjusted based on the estimated rRNA operon copy number according to the rrnDB database [62].

Metagenomic sequencing and analysis

DNA extract was fragmented to an average size of about 400 bp by Covaris M220 (Gene Company Limited, P. R. China) for paired-end library construction. The paired-end library was built using NEXTFLEX Rapid DNA-Seq (Bioo Scientific, Austin, TX, USA). Paired-end sequencing was conducted on Illumina Novaseq 6000 (Illumina Inc., San Diego, CA, USA) using NovaSeq 6000 S4 Reagent Kit according to the manufacturer's instructions (www.illumina.com). Fastp (https://github.com/OpenGene/fastp, version 0.20.0) was used to trim the raw sequencing reads and remove low-quality reads (length $<$ 50 bp or with a quality value $<$ 20 or having N bases). Reads associated with the *bos taurus* genome were removed. The quality-filtered data were assembled using MEGAHIT (https://github.com/voutcn/megahit, version 1.1.2). We chose contigs with a length $\geq$ 300 bp as the final assembling result and used Prodigal (https://github.com/hyattpd/Prodigal, version2.6.3) to predict open reading frames (ORFs) from each assembled contigs. Moreover, the length $\geq$ 100 bp ORFs were retrieved. The CD-HIT (http://weizhongli-lab.org/cd-hit/, version 4.7) with 90% sequence identity and 90% coverage was applied to construct the non-redundant gene catalog. We also estimated gene abundance for a certain sample according to SOAPaligner (https://github.com/ShujiaHuang/SOAPaligner, version soap2.21 release) with 95% identity. We aligned them against the NCBI NR database by DIAMOND (http://ab.inf.uni-tuebingen.de/software/diamond/, version 2.0.11) with an e-value cutoff of 1e − 5 to obtain the best-hit taxonomy of non-redundant genes Similarly, the functional annotation (KEGG and CAZy,) of non-redundant genes was also obtained [63].

Metabolite extraction and quality control

We added 50 mg fecal sample to a 2-mL centrifuge tube followed by a 6-mm diameter grinding bead. The samples were ground by the Wonbio-96c (Shanghai Wanbo Biotechnology Co., LTD) frozen tissue grinder for 6 min (− 10 °C, 50 Hz) and extracted for 30 min (5 °C, 40 kHz) using low-temperature ultrasonic. After being left at − 20 °C for 30 min and centrifuged for 15 min (4 °C, 13,000 × *g*), the supernatant of samples was collected for the next analysis. The QC samples (mixed by equal volumes of all samples) were made to monitor the stability of the analysis.

Metabolomics data analysis

The LC–MS/MS analysis of the sample was conducted on a Thermo UHPLC-Q Exactive HF-X system equipped with an ACQUITY HSS T3 column (100 mm × 2.1 mm i.d., 1.8 µm; Waters, USA). Under both positive and negative ion modes, The TripleTOF 5600 Plus high-resolution tandem mass spectrometer (SCIEX, Warrington, UK) was performed to identify metabolites eluted from the column. The acquired data were exported into the mzXML format using XCMS software [64]. The analysis of traceability and enrichment of metabolites was performed using MetOrigin (http://metorigin.met-bioinformatics.cn/app/metorigin). On MetOrigin online server, the Simple MetOrigin Analysis (SMOA) mode that requires a list of metabolites with KEGG or HMDB IDs was chosen for our data. SMOA provides origin analysis to identify the origins of metabolites based on seven well-known metabolite databases. After the loaded dataset, the MPEA analysis was carried out. As a result, a bar plot was produced to summarize the total number of metabolites from the host, microbiota, co-metabolism, and others.

The analysis of serum samples

Serum was used to analyze several factors including GLU, TP, ALB, UREA, T-SOD, T-AOC, GSH, GSH-PX, MDA, NEFA, IL-1β, IL-6, TNF-α, IGF-1 and BHBA. GLU, TP, ALB, and UREA concentrations were measured using an automated biochemistry analyzer from Shanghai Kehua Biological Engineering Co., Ltd., Shanghai, P. R. China. The concentration of T-SOD, T-AOD, GSH-PX, MDA, NEFA, IL-1β, IL-6, TNF-α, IGF-1, and BHBA was measured using kits from Shanghai Huole Biotechnological Science and Technology Co. Ltd., Shanghai, P. R. China.

Isolation and identification of Bifidobacterium

The cow feces of cluster2 were thawed at room temperature and vortexed for 1 min in an anaerobic workstation until it was mixed. Subsequently, 1 mL of fecal sample was pipetted into 9 mL of normal saline, mixed to a 10^{-1} dilution, and then further diluted to a 10^{-5} dilution in a gradient manner. The diluent was added to the modified Man Rogosa Sharpe Medium (MRS) liquid medium (100 μl/dish) and applied evenly. After the surface of the plate was dried, the plate was upside down and cultured at 37 ℃ for 3 to 5 days. The growth status of the isolated culture medium was continuously observed and the single colony was selected with a sterilized toothpick to purify the strain, followed by pure culture (Fig. S8A). The 16S rRNA gene sequencing was applied to identify the strain. As a result, a strain of *B. longum* (named *B. longum 1109*) was successfully isolated from cow feces of cluster 2. Then, the *B. longum 1109* was cultured using the MRS in the micro-anaerobic incubation tank to collect sufficient and vigorous cultures of the target strain (Fig. S8B). In the anaerobic workstation, the expanded cultured bacterial liquid was poured into a centrifugal cup and centrifuged under the condition at 4500 r/min for 10–15 min. After centrifugation, the supernatant was discarded and the bacteria were collected. Finally, the strain was diluted and counted according to the basic microbial operation technology. When the number of bacteria stabilized at 1×10^8 colony-forming units, the bacterial liquid was collected in a sterile test tube and added with glycerol protective solution (Glycerol: PBS = 1:3) and stored in a minus 80 refrigerator for the next mice experiment.

Mice experimental design

A total of 20, 3-week-old female specific pathogen-free (SPF) C57BL/6 J mice (Sibeifu Biotechnology Co., Ltd., Beijing, China) were enrolled in the experiment and underwent a 7-day acclimatization stage before treatment. All the mice were kept in the SPF animal barrier facilities and fed with a normal diet (AIN-93G; Table S5) and purified water. The feeding conditions were room temperature (23.0 ± 2.0 ℃), relative humidity of 50–60%, and 12 h of light every day. Next, the mice were treated with an antibiotics cocktail (ampicillin 1 g/L, neomycin 1 g/L, metronidazole 1 g/L, vancomycin 0.5 g/L, diluted in ultra-pure water) for 7 days to deplete the gut microbiome. In detail, the mice had unrestricted access to antibiotics cocktail water and also administered an additional 200 μL/day of antibiotics cocktail. After 7 days, the mice experienced a 4-day wash-out period [65–67] to eliminate the residual antibiotics before *B. longum 1109* administration. Subsequently, these mice were randomly divided into 2 groups ($n = 10$; 5 mice/cage; CON and TRT), which were colonized by oral gavage with 200 μL/day of PBS or *B. longum 1109* for 2 weeks. During the period, we measured the weight of the mice every day, and at the end of 14 days, all the mice we euthanized. The colonic tissues of mice were collected to make the paraffin sections for subsequent histological observation. The blood samples were also obtained for the serological test.

Histomorphologic examinations

Colonic tissue samples were dehydrated in a series of ethanol solutions, embedded in paraffin sections, and cut into 6 μm sections. The sections were stained with hematoxylin, and the colonic structure was observed under an Olympus BX-51 light microscope (Olympus Corporation, Tokyo, Japan) at × 20 magnification. The microscopic evaluations were conducted blindly by an experienced pathologist.

Statistics

Phenotypic clustering of calves was performed using k-means clustering analysis. The optimal number of clusters was determined by calculating the silhouette coefficient using the “factoextra” package in R (version 4.2.3). After clustering, the “FeatureImpCluster” package was used to calculate the importance of the variables within the clustering results.

The difference in growth performance and serum indicator level in calves between the two clusters was conducted using one-way ANOVA in SPSS software (version 25, SPSS Inc., Chicago, IL, USA). Differences of $P < 0.05$ were considered significant. The package of “psych” in R (version 4.2.3) was used to calculate Spearman’s correlations between gut microbiota and apparent factors.

Wilcoxon rank-sum test was applied to compare the difference of alpha diversity (Shannon Index and Chao1), microbial abundance, and GHs abundance, and related bar charts were visualized by GraphPad Prism (version 3.7.1), Differences of $P < 0.05$ were considered significant.

Beta diversity based on Bray–Curtis distances was calculated and tested using an analysis of similarity (ANOSIM). The LEfSe was used to identify the signature microbiota and microbial functions. LDA scores > 3 and

$P < 0.05$ were used as a criterion for judging the significant effect size.

The genera with an average abundance of greater than 0.01% were retained for the network analysis. The package of "psych" in R (version 4.2.3) was used to calculate the correlations between bacteria by Spearman analysis and only the robust correlations identified by $P < 0.05$ and $R > 0.5$ were applied to construct the network. The networks were visualized by Cytoscape (version 3.7.1, Bethesda, MD, USA). MCODE plugin in Cytoscape (version 2.0, http://apps.cytoscape.org/apps/mcode) was chosen to identify the core sub-network with programmed parameters (degree cutoff: 2; K-Core: 2; and max depth: 100).

Supplementary Information

The online version contains supplementary material available at https://doi.org/10.1186/s40168-024-02010-9.

Supplementary Material 1. Figure S1. The comparison of bacterial abundance between the two clusters. **A** The comparison of microbiota at the phylum level. **B** The comparison of microbiota at the genus level. Figure S2. Procrustes analysis for consistency between phenotype and gut microbiology. Figure S3. Principal coordinate analysis of the gut bacterial species in cluster1 and cluster2. Figure S4. Differences in metabolic function at KEGG level2 between the cluster1 and cluster2. Figure S5. Differences in the abundance of genes of Carbohydrate-active enzymes (CAZymes) in cluster1 and cluster2. **A** Relative abundance of total CAZymes genes. **B** The principal coordinate analysis (PCoA) of the GH families in the cluster1 and cluster2. **C** Differences in the abundance of dominant GH members between the cluster1 and cluster2. Figure S6. Microbiome and host Wayne diagram. Figure S7 The colon length of mice in the CON and TRT group. Figure S8. The process of isolation and culture of *B. longum 1109*. A The Growth status of *B. longum 1109* in anaerobic blood plate (24 hours). B Dilution and coating culture of *B. longum 1109* fermentation broth. Table S1. Descriptive statistics of phenotypic indicators for cluster1 and cluster2. Table S2. Comparative analysis of the indicators in the cluster1 and cluster2. Table S3. The liquid feed regime of calves. Table S4. Nutritional components of calf feed. Table S5. Ingredients and nutritional components of mice diet.

Acknowledgements
We thank Mei Ma, Jiaying Ma, Xiaotong Kang, Shuangyi Wang, and Tianhao Dong from China Agricultural University (Beijing, P. R. China) for their kind help during this study.

Authors' contributions
Z.C. served as the principal investigator. M.L., W.W., and S.L. designed the experiments. Y. Z., W. J., and D.G. analyzed metagenomic data, and 16S rRNA gene sequencing and drafted the manuscript. S. L., Y. X., T. C., J. X., S. L., G. H., G. L., and S. Z. contributed to the collection of samples. All authors discussed the results, critically reviewed the text, and approved the final manuscript.

Funding
This work has been supported by grants from the Key Research and Development Program of Ningxia (2024BBF01006), the National Natural Science Foundation of China (32272902), and the China National Postdoctoral Program for Innovative Talents (BX20230419).

Data availability
The accession for the 16s rRNA gene sequencing and metagenomic data in this study are in the NCBI Sequence Read Archive: # PRJNA1052964.

Declarations

Ethics approval and consent to participate
The animal care protocol was approved by the Animal Care and Use Committee of China Agricultural University (Protocol Number: AW10803202-3-2).

Consent for publication
Not applicable.

Competing interests
The authors declare that they have no competing interests.

Author details
[1]State Key Laboratory of Animal Nutrition and Feeding, International Calf and Heifer Organization, College of Animal Science and Technology, China Agricultural University, Beijing 100193, China. [2]College of Animal Science, Xinjiang Uygur Autonomous Region 830052, Xinjiang Agricultural University, Urumqi, China. [3]Animal Nutrition Institute, Sichuan Agricultural University, Chengdu 611130, China. [4]College of Animal Science and Technology, Beijing University of Agriculture, Beijing 102206, China.

Received: 12 June 2024 Accepted: 17 December 2024
Published online: 16 January 2025

References
1. Zanton GI, Heinrichs AJ. Meta-analysis to assess effect of prepubertal average daily gain of Holstein heifers on first-lactation production. J Dairy Sci. 2005;88(11):3860–7.
2. Wang D, Chen L, Tang G, Yu J, Chen J, Li Z, Cao Y, Lei X, Deng L, Wu S, et al. Multi-omics revealed the long-term effect of ruminal keystone bacteria and the microbial metabolome on lactation performance in adult dairy goats. Microbiome. 2023;11(1):215.
3. Gelsinger SL, Heinrichs AJ, Jones CM. A meta-analysis of the effects of preweaned calf nutrition and growth on first-lactation performance. J Dairy Sci. 2016;99(8):6206–14.
4. Chai J, Lv X, Diao Q, Usdrowski H, Zhuang Y, Huang W, Cui K, Zhang N. Solid diet manipulates rumen epithelial microbiota and its interactions with host transcriptomic in young ruminants. Environ Microbiol. 2021;23(11):6557–68.
5. Zhao C, Bao L, Qiu M, Wu K, Zhao Y, Feng L, Xiang K, Zhang N, Hu X, Fu Y. Commensal cow Roseburia reduces gut-dysbiosis-induced mastitis through inhibiting bacterial translocation by producing butyrate in mice. Cell Rep. 2022;41(8): 111681.
6. Cho I, Blaser MJ. The human microbiome: at the interface of health and disease. Nat Rev Genet. 2012;13(4):260–70.
7. Wastyk HC, Fragiadakis GK, Perelman D, Dahan D, Merrill BD, Yu FB, Topf M, Gonzalez CG, Van Treuren W, Han S *et al*: Gut-microbiota-targeted diets modulate human immune status. *Cell* 2021, 184(16):4137–4153 e4114.
8. Wang D, Tang G, Zhao L, Wang M, Chen L, Zhao C, Liang Z, Chen J, Cao Y, Yao J. Potential roles of the rectum keystone microbiota in modulating the microbial community and growth performance in goat model. J Anim Sci Biotechnol. 2023;14(1):55.
9. Li QS, Wang R, Ma ZY, Zhang XM, Jiao JZ, Zhang ZG, Ungerfeld EM, Yi KL, Zhang BZ, Long L, et al. Dietary selection of metabolically distinct microorganisms drives hydrogen metabolism in ruminants. Isme j. 2022;16(11):2535–46.
10. Gu F, Zhu S, Tang Y, Liu X, Jia M, Malmuthuge N, Valencak TG, McFadden JW, Liu JX, Sun HZ. Gut microbiome is linked to functions of peripheral immune cells in transition cows during excessive lipolysis. Microbiome. 2023;11(1):40.
11. Gu F, Zhu S, Hou J, Tang Y, Liu JX, Xu Q, Sun HZ. The hindgut microbiome contributes to host oxidative stress in postpartum dairy cows by affecting glutathione synthesis process. Microbiome. 2023;11(1):87.
12. Zhang MQ, Heirbaut S, Jing XP, Stefańska B, Vandaele L, De Neve N, Fievez V. Transition cow clusters with distinctive antioxidant ability and their relation to performance and metabolic status in early lactation. J Dairy Sci. 2023;106(8):5723–39.

13. Bader GD, Hogue CW. An automated method for finding molecular complexes in large protein interaction networks. BMC Bioinformatics. 2003;4:2.
14. Seshadri R, Leahy SC, Attwood GT, Teh KH, Lambie SC, Cookson AL, Eloe-Fadrosh EA, Pavlopoulos GA, Hadjithomas M, Varghese NJ, et al. Cultivation and sequencing of rumen microbiome members from the Hungate1000 Collection. Nat Biotechnol. 2018;36(4):359–67.
15. Yu G, Xu C, Zhang D, Ju F, Ni Y: MetOrigin: Discriminating the origins of microbial metabolites for integrative analysis of the gut microbiome and metabolome. *iMeta* 2022, 1:e10.
16. Marcato F, van den Brand H, Hoorweg FA, Bruckmaier RM, Gross JJ, Schnabel SK, Wolthuis-Fillerup M, van Reenen K. Effects of transport age (14 versus 28 days of age) on blood total cholesterol, insulin, and insulin-like growth factor-1 concentrations of veal calves. J Dairy Sci. 2024;107(8):6104–16.
17. Haisan J, Oba M, Ambrose DJ, Steele MA. Short communication: the effects of offering a high or low plane of milk preweaning on insulin-like growth factor and insulin-like growth factor binding proteins in dairy heifer calves. J Dairy Sci. 2018;101(12):11441–6.
18. Wilms JN, Ghaffari MH, Steele MA, Sauerwein H, Martín-Tereso J, Leal LN. Macronutrient profile in milk replacer or a whole milk powder modulates growth performance, feeding behavior, and blood metabolites in ad libitum-fed calves. J Dairy Sci. 2022;105(8):6670–92.
19. Park P, Cohen P. The role of insulin-like growth factor I monitoring in growth hormone-treated children. Horm Res. 2004;62(Suppl 1):59–65.
20. Walenkamp MJ, Losekoot M, Wit JM. Molecular IGF-1 and IGF-1 receptor defects: from genetics to clinical management. Endocr Dev. 2013;24:128–37.
21. Yanar KE, Gür C, Değirmençay Ş, Aydın Ö, Aktaş MS, Baysal S. Insulin-like growth factor-1 expression levels in pro-inflammatory response in calves with neonatal systemic inflammatory response syndrome. Vet Immunol Immunopathol. 2024;268: 110706.
22. Shakeri F, Kiani S, Rahimi G, Boskabady MH: Anti-inflammatory, anti-oxidant, and immunomodulatory effects of Berberis vulgaris and its constituent berberine, experimental and clinical, a review. *Phytother Res : PTR* 2024.
23. Cai S, Sun Y, Wang Y, Lin Z. Exploring the effect of LncRNA DANCR to regulate the Keap1-Nrf2/ARE pathway on oxidative stress in rheumatoid arthritis. Immun Inflamm Dis. 2024;12(1): e1163.
24. Guo C, Wang X, Dai D, Kong F, Wang S, Sun X, Li S, Xu X, Zhang L. Effects of alkaline mineral complex supplementation on production performance, serum variables, and liver transcriptome in calves. Front Vet Sci. 2023;10:1282055.
25. Hizo GH, Rampelotto PH. The Impact of Probiotic Bifidobacterium on Liver Diseases and the Microbiota. Life (Basel, Switzerland). 2024;14(2):239.
26. Wang H, Huang X, Tan H, Chen X, Chen C, Nie S. Interaction between dietary fiber and bifidobacteria in promoting intestinal health. Food Chem. 2022;393: 133407.
27. Derrien M, Turroni F, Ventura M, van Sinderen D. Insights into endogenous Bifidobacterium species in the human gut microbiota during adulthood. Trends Microbiol. 2022;30(10):940–7.
28. D'Aimmo MR, Mattarelli P, Biavati B, Carlsson NG, Andlid T. The potential of bifidobacteria as a source of natural folate. J Appl Microbiol. 2012;112(5):975–84.
29. Kim G, Yoon Y, Park JH, Park JW, Noh MG, Kim H, Park C, Kwon H, Park JH, Kim Y, et al. Bifidobacterial carbohydrate/nucleoside metabolism enhances oxidative phosphorylation in white adipose tissue to protect against diet-induced obesity. Microbiome. 2022;10(1):188.
30. Xiao Y, Yang C, Yu L, Tian F, Wu Y, Zhao J, Zhang H, Yang R, Chen W, Hill C *et al*: Human gut-derived B. longum subsp. longum strains protect against aging in a D-galactose-induced aging mouse model. *Microbiome* 2021, 9(1):180.
31. Martín R, Rios-Covian D, Huillet E, Auger S, Khazaal S, Bermúdez-Humarán LG, Sokol H, Chatel JM, Langella P: Faecalibacterium: a bacterial genus with promising human health applications. *FEMS Microbiol Rev* 2023, 47(4):fuad039.
32. Lopez-Siles M, Martinez-Medina M, Abellà C, Busquets D, Sabat-Mir M, Duncan SH, Aldeguer X, Flint HJ, Garcia-Gil LJ. Mucosa-associated Faecalibacterium prausnitzii phylotype richness is reduced in patients with inflammatory bowel disease. Appl Environ Microbiol. 2015;81(21):7582–92.
33. Wrzosek L, Miquel S, Noordine ML, Bouet S, Joncquel Chevalier-Curt M, Robert V, Philippe C, Bridonneau C, Cherbuy C, Robbe-Masselot C, et al. Bacteroides thetaiotaomicron and Faecalibacterium prausnitzii influence the production of mucus glycans and the development of goblet cells in the colonic epithelium of a gnotobiotic model rodent. BMC Biol. 2013;11:61.
34. Lindstad LJ, Lo G, Leivers S, Lu Z, Michalak L, Pereira GV, Røhr Å K, Martens EC, McKee LS, Louis P *et al*: Human gut faecalibacterium prausnitzii deploys a highly efficient conserved system to cross-feedon β-Mannan-derived oligosaccharides. *mBio* 2021, 12(3):e0362820.
35. Devriese S, Eeckhaut V, Geirnaert A, Van den Bossche L, Hindryckx P, Van de Wiele T, Van Immerseel F, Ducatelle R, De Vos M, Laukens D. Reduced mucosa-associated butyricicoccus activity in patients with ulcerative colitis correlates with aberrant claudin-1 expression. J Crohns Colitis. 2017;11(2):229–36.
36. Dempsey E, Corr SC: Lactobacillus spp. for gastrointestinal health: current and future perspectives. *Front Immunol* 2022, 13:840245.
37. Peng Z, Wei B, Huang T, Liu Z, Guan Q, Xie M, Li H, Xiong T. Screening, safety evaluation, and mechanism of two lactobacillus fermentum strains in reducing the translocation of staphylococcus aureus in the Caco-2 monolayer model. Front Microbiol. 2020;11: 566473.
38. Röttjers L, Faust K. From hairballs to hypotheses–biological insights from microbial networks. FEMS Microbiol Rev. 2018;42(6):761–80.
39. Zhuang Y, Guo W, Cui K, Tu Y, Diao Q, Zhang N, Bi Y, Ma T: Altered microbiota, antimicrobial resistance genes, and functional enzyme profiles in the rumen of yak calves fed with milk replacer. *Microbiol Spectr* 2023, 0(0):e01314–01323.
40. Zhuang Y, Chai J, Cui K, Bi Y, Diao Q, Huang W, Usdrowski H, Zhang N. **Lo**ngitudinal investigation of the gut microbiota in goat kids from birth to postweaning. Microorganisms. 2020;8(8):1111.
41. Milani C, Turroni F, Duranti S, Lugli GA, Mancabelli L, Ferrario C, van Sinderen D, Ventura M. Genomics of the genus bifidobacterium reveals species-specific adaptation to the glycan-rich gut environment. Appl Environ Microbiol. 2016;82(4):980–91.
42. Watanabe Y, Saito Y, Hara T, Tsukuda N, Aiyama-Suzuki Y, Tanigawa-Yahagi K, Kurakawa T, Moriyama-Ohara K, Matsumoto S, Matsuki T. Xylan utilisation promotes adaptation of Bifidobacterium pseudocatenulatum to the human gastrointestinal tract. ISME Commun. 2021;1(1):62.
43. Wardman JF, Bains RK, Rahfeld P, Withers SG. Carbohydrate-active enzymes (CAZymes) in the gut microbiome. Nat Rev Microbiol. 2022;20(9):542–56.
44. Tropak MB, Reid SP, Guiral M, Withers SG, Mahuran D. Pharmacological Enhancement of β-Hexosaminidase Activity in Fibroblasts from Adult Tay-Sachs and Sandhoff Patients. J Biol Chem. 2004;279(14):13478–87.
45. Koshland DE, Stein SS. Correlation of bond breaking with enzyme specificity; cleavage point of invertase. J Biol Chem. 1954;208(1):139–48.
46. Di Lauro B, Strazzulli A, Perugino G, La Cara F, Bedini E, Corsaro MM, Rossi M, Moracci M. Isolation and characterization of a new family 42 β-galactosidase from the thermoacidophilic bacterium Alicyclobacillus acidocaldarius: Identification of the active site residues. Biochim Biophys Acta. 2008;1784(2):292–301.
47. Henrissat B, Claeyssens M, Tomme P, Lemesle L, Mornon JP. Cellulase families revealed by hydrophobic cluster analysi. Gene. 1989;81(1):83–95.
48. Kimura I, Miyamoto J, Ohue-Kitano R, Watanabe K, Yamada T, Onuki M, Aoki R, Isobe Y, Kashihara D, Inoue D *et al*: Maternal gut microbiota in pregnancy influences offspring metabolic phenotype in mice. *Science* 2020, 367(6481):eaaw8429.
49. Zheng H, Xu P, Jiang Q, Xu Q, Zheng Y, Yan J, Ji H, Ning J, Zhang X, Li C, et al. Depletion of acetate-producing bacteria from the gut microbiota facilitates cognitive impairment through the gut-brain neural mechanism in diabetic mice. Microbiome. 2021;9(1):145.
50. Louis P, Flint HJ. Formation of propionate and butyrate by the human colonic microbiota. Environ Microbiol. 2017;19(1):29–41.
51. Yin P, Du T, Yi S, Zhang C, Yu L, Tian F, Chen W, Zhai Q. Response differences of gut microbiota in oligofructose and inulin are determined by the initial gut Bacteroides/Bifidobacterium ratios. Food Res Int. 2023;174(Pt 1): 113598.
52. Wei X, Li D, Feng C, Mao H, Zhu J, Cui Y, Yang J, Gao H, Wang C. Effects of hydrogen peroxide and l-tryptophan on antioxidative potential,

apoptosis, and mammalian target of rapamycin signaling in bovine intestinal epithelial cells. J Dairy Sci. 2022;105(12):10007–19.
53. Yeste N, Bassols A, Vidal M, Bach A, Terré M. Evaluating the potential role of tryptophan in calf milk replacers to facilitate weaning. J Dairy Sci. 2020;103(8):7009–17.
54. Wu S, Liu X, Cheng L, Wang D, Qin G, Zhang X, Zhen Y, Wang T, Sun Z. Protective Mechanism of Leucine and Isoleucine against H(2)O(2)-Induced Oxidative Damage in Bovine Mammary Epithelial Cells. Oxid Med Cell Longev. 2022;2022:4013575.
55. Kim HS, Whon TW, Sung H, Jeong YS, Jung ES, Shin NR, Hyun DW, Kim PS, Lee JY, Lee CH, et al. Longitudinal evaluation of fecal microbiota transplantation for ameliorating calf diarrhea and improving growth performance. Nat Commun. 2021;12(1):161.
56. Luo YH, Su Y, Wright AD, Zhang LL, Smidt H, Zhu WY. Lean breed Landrace pigs harbor fecal methanogens at higher diversity and density than obese breed Erhualian pigs. Archaea. 2012;2012: 605289.
57. Chen M, Yao H, Tan H, Huang W, Wu Q, Nie S. Impact of Bifidobacterium longum NSP001 on DSS-induced colitis in conventional and humanised mice. Food Sci Hum Wellness. 2023;12(4):1109–18.
58. Zhu G, Guo M, Zhao J, Zhang H, Wang G, Chen W. Environmental enrichment in combination with Bifidobacterium breve HNXY26M4 intervention amplifies neuroprotective benefits in a mouse model of Alzheimer's disease by modulating glutamine metabolism of the gut microbiome. Food Sci Hum Wellness. 2024;13(2):982–92.
59. Lee SH, Cho SY, Yoon Y, Park C, Sohn J, Jeong JJ, Jeon BN, Jang M, An C, Lee S, et al. Bifidobacterium bifidum strains synergize with immune checkpoint inhibitors to reduce tumour burden in mice. Nat Microbiol. 2021;6(3):277–88.
60. Larson LL, Owen FG, Albright JL, Appleman RD, Lamb RC, Muller LD. Guidelines Toward More Uniformity in Measuring and Reporting Calf Experimental Data1. J Dairy Sci. 1977;60(6):989–91.
61. Chen S, Zhou Y, Chen Y, Gu J. fastp: an ultra-fast all-in-one FASTQ preprocessor. Bioinformatics. 2018;34(17):i884–90.
62. Stoddard SF, Smith BJ, Hein R, Roller BR, Schmidt TM: rrnDB: improved tools for interpreting rRNA gene abundance in bacteria and archaea and a new foundation for future development. *Nucleic Acids Res* 2015, 43(Database issue):D593–598.
63. Buchfink B, Xie C, Huson DH. Fast and sensitive protein alignment using DIAMOND. Nat Methods. 2015;12(1):59–60.
64. Gowda H, Ivanisevic J, Johnson CH, Kurczy ME, Benton HP, Rinehart D, Nguyen T, Ray J, Kuehl J, Arevalo B, et al. Interactive XCMS Online: simplifying advanced metabolomic data processing and subsequent statistical analyses. Anal Chem. 2014;86(14):6931–9.
65. Ni Y, Qian L, Siliceo SL, Long X, Nychas E, Liu Y, Ismaiah MJ, Leung H, Zhang L, Gao Q, et al. Resistant starch decreases intrahepatic triglycerides in patients with NAFLD via gut microbiome alterations. Cell Metab. 2023;35(9):1530-1547.e1538.
66. Hoyles L, Fernández-Real JM, Federici M, Serino M, Abbott J, Charpentier J, Heymes C, Luque JL, Anthony E, Barton RH, et al. Molecular phenomics and metagenomics of hepatic steatosis in non-diabetic obese women. Nat Med. 2018;24(7):1070–80.
67. Liu Y, Wang Y, Ni Y, Cheung CKY, Lam KSL, Wang Y, Xia Z, Ye D, Guo J, Tse MA, et al. **G**ut microbiome fermentation determines the efficacy of exercise for diabetes prevention. Cell Metab. 2020;31(1):77-91.e75.

Publisher's Note